



**CR-ICP-2007-2012 (DECC, Defra & MoD)
DECC/Defra(GA01101), MoD(CBC/2B/0417_Annex C5)**

**Integrated Climate Programme (ICP) 2007-2012
Output Product Cover Sheet**

Product Number: M3.2

Product Title: Comparison between UKCA-MODE and CLASSIC aerosol schemes in HadGEM3

Product Author(s) and Team: C.E. Johnson, G.W. Mann¹, N. Bellouin, F.M. O'Connor, and M. Dalvi – Climate, Chemistry and Ecosystems

¹Institute of Atmospheric Sciences, Leeds University

Delivered from authors:	Signature	Colin Johnson	Date 8.3.10
Scientific content approved by activity manager:	Signature	Olivier Boucher	Date 8.3.10
Approved by HdCCA against customer requirements:	Signature	Vicky Pope	Date 8.3.10
Sent to DECC, Defra, & MoD:	Signature	Linda Livingston	Date 8.3.10

Version Number: 3

No of pages: 23

Security Classification: Unclassified

File Reference: M/DoE/2/9

Key outcomes/non technical summary

- 1) Two aerosol schemes operating within the HadGEM3 climate model are compared. These are I) the CLASSIC aerosol scheme previously used in Hadley Centre Climate Models; and II) the new UKCA-MODE aerosol scheme.
- 2) Sulphate aerosol in UKCA-MODE is higher than in CLASSIC for high latitudes, especially in the northern hemisphere. This is attributed to the lack of the dimethylsulphide plus nitrate radical oxidation reaction in the CLASSIC model, and a longer lifetime for sulphate in UKCA-MODE.
- 3) The global, annual average aerosol optical depth simulated at $0.55 \mu\text{m}$ is around 10 % higher for UKCA-MODE than for CLASSIC, and this gives an improved comparison against satellite retrievals, notably over the continental areas of the northern hemisphere. Seasonal root mean square error between simulated and measured (AERONET) AOD was consistently lower for UKCA-MODE than for CLASSIC.
- 4) The short-wave direct radiative effect of the aerosol at the top of the atmosphere is estimated to be $-2.4 \pm 0.1 \text{ Wm}^{-2}$ for UKCA-MODE and $-2.0 \pm 0.2 \text{ Wm}^{-2}$ for CLASSIC. The radiative forcing exerted per unit aerosol optical depth was similar for both models at -30.8 and -30.1 Wm^{-2} respectively. The similarity between these numbers lends confidence to the direct radiative forcing calculations.
- 5) This intercomparison between aerosol models using the latest emission datasets prepared for the IPCC simulations has produced the best set of results to date from UKCA-MODE as assessed against observations. The intercomparison with CLASSIC and other models is also good, but shows differences in the sulphur oxidation and aerosol wet removal processes. More work is needed in these areas to improve consistency between models and observations.
- 6) The main improvement of the UKCA-MODE model is expected to be in the simulation of aerosol number. This is crucial to enable better estimates of aerosol indirect effects on clouds and precipitation, and the comparison of predicted cloud condensation nuclei with observations shows improvement over the results from the CLASSIC model.
- 7) Development of UKCA-MODE is proceeding, with ongoing work on mineral dust, ammonium, and nitrate components, as well as the prediction of indirect effects on clouds and precipitation.

Associated publications

Press interest

None.

Contents

1	Introduction	3
2	Model Description	3
2.1	The HadGEM3 Climate Model	3
2.2	CLASSIC Aerosol Scheme	4
2.3	UKCA-MODE Aerosol Scheme	4
2.4	Direct Radiative Effect and Forcing	5
3	Experimental Design	7
4	Results	7
4.1	Atmospheric gas-phase constituents	7
4.2	Sulphur oxidation and sulphate aerosol concentrations	10
4.3	Speciated aerosol mass and lifetime	12
4.4	Comparison between aerosol optical depths	13
4.5	Comparison of direct radiative effect	16
4.6	Number concentrations	19
5	Conclusions	19

1 Introduction

Uncertainties in radiative forcing from aerosols are documented in the IPCC Fourth Assessment Report (Solomon et al., 2007). The contribution to the overall uncertainty from aerosol components remains high, and this is the key reason driving the development of better aerosol models. Anderson et al. (2005) discuss the uncertainties in direct climate forcing from aerosols, and consider that these uncertainties could be substantially reduced by utilising satellite and other recent measurements to constrain and validate model predictions. Clearly, improvements to modelling aerosol processes are important, and the UKCA-MODE aerosol scheme offers clear advantages over older schemes, notably by treating both aerosol number and mass concentrations as prognostic variables.

Here we investigate the differences in aerosol mass, optical depth and direct radiative forcing from two models which predict aerosols operating within the same climate model.

2 Model Description

2.1 The HadGEM3 Climate Model

The United Kingdom Chemistry and Aerosol (UKCA) model has been coupled to the HadGEM3 Hadley Centre climate model, which is based on the Met Office Unified Model (MetUM). HadGEM3 is being developed with a variety of resolutions, here the horizontal latitude-longitude grid in use is a staggered Arakawa C-grid (Arakawa and Lamb 1977) with a resolution of N96 (1.25° latitude x 1.875° longitude). A staggered

Charney-Phillips grid is used in the vertical with 38 levels extending up to 39 km. The dynamical timestep corresponding to this resolution is 30 minutes. The configuration used for the integrations described here was the atmosphere-only version of HadGEM3, with sea-surface temperatures and sea-ice prescribed as seasonally varying fields. Coupled within the climate model, UKCA uses components of the MetUM for the large-scale advection, convective transport, and boundary layer mixing of its chemical tracers. The large-scale transport is based on the new dynamical core implemented in the MetUM by Davies et al. (2005). Advection is semi-Lagrangian with conservative and monotone treatment of tracers. Convective transport is treated according to the mass-flux scheme of Gregory and Rowntree (1990) and is applicable to moist convection of all types (shallow, deep, and mid-level) in addition to dry convection. For boundary layer mixing, UKCA uses a new boundary layer turbulent mixing scheme (Lock et al. 2000) which includes a representation of non-local mixing in unstable layers and an explicit entrainment parameterization.

2.2 CLASSIC Aerosol Scheme

The aerosol scheme used in previous Hadley Centre climate models is called CLASSIC (Coupled Large-scale Aerosol Simulator for Studies In Climate), and is described by Jones et al. (2001). Improvements to this scheme for the HadGEM2 climate model are documented in Bellouin et al. (2007) and Rae et al. (2007). Recently, new aerosol species to represent organic carbon derived from fossil-fuel burning, and ammonium nitrate have been added to the scheme. The ammonium nitrate scheme is not used here to maintain consistency with the aerosol species represented in MODE. The CLASSIC scheme represents the mass of each aerosol species by a single log-normal mode, described by an appropriate modal radius and geometric standard deviation. Species are represented as the mass in two modes together with, for soluble species, another tracer to represent the aerosol mass incorporated into cloud water. The two modes represent either different size classes or (for black carbon and biomass) fresh or aged aerosol. Table 1 summarises the species and modes included in CLASSIC together with their assumed modal radius.

Two aerosol species are represented rather differently: sea-salt is parameterised as a function of near-surface wind speed over the ocean, and is not treated as a tracer; and mineral dust is modelled in six bins in order to treat the wide range of size classes encountered. The mineral dust scheme is described by Woodward (2001).

2.3 UKCA-MODE Aerosol Scheme

The UKCA-MODE aerosol scheme uses a two-moment modal scheme where both the particle number density and the species mass are carried as prognostic tracers. The model framework follows that of the M7 model (Vignati et al., 2004), and table 2 shows the components and modes used by UKCA-MODE. The model contains a description of aerosol microphysics including nucleation of sulphuric acid, condensation, coagulation and cloud processing. Direct emissions of sulphate, black-carbon, and organic carbon are included, and secondary aerosol production from sulphur and terpene oxidation is taken into account. Aerosol removal by dry and wet deposition is also included. Dust and ammonium nitrate are not yet represented in the UKCA-MODE model.

Species name	Modal Radius (μm)	Hygroscopic ?
Aitken sulphate	0.0065	Yes
Accumulation sulphate	0.095	Yes
Fresh black-carbon	0.04	No
Aged black-carbon	0.04	No
Sea-salt film	0.1	Yes
Sea-salt jet	1.0	Yes
Fresh biomass	0.1	Yes
Aged biomass	0.12	Yes
Fresh fossil-fuel OC	0.1	Yes
Aged fossil-fuel OC	0.12	Yes

Table 1: CLASSIC aerosol scheme, with component species. In addition to the species listed here, dust is modelled in six divisions, and some species (sulphate, black-carbon, biomass and fossil-fuel organic carbon (OC)) are modelled with a dissolved mode.

The absorption and scattering of solar radiation by aerosol depends on having an accurate estimate of the water content of the aerosol due to hygroscopic uptake (e.g. Tang and Munkelwitz, 1994). In contrast to CLASSIC, the model assumes an internal mixture of the soluble aerosol components, and the water content is evaluated within this assumption using the ZSR algorithm (Stokes and Robinson, 1966), using water activity data from Jacobson et al. (1996).

UKCA-MODE has been developed in an off-line chemical transport model TOMCAT, and has been ported to the MetUM to form a component of the UKCA model. A brief description of the TOMCAT version is available (Manktelow et al., 2007), and a fuller description is in preparation (Mann et al., 2010).

UKCA-MODE is integrated with a tropospheric chemistry scheme which describes the inorganic chemistry of O_x - NO_x - HO_x -CO chemistry, together with near-explicit degradation schemes for methane, ethane, propane, and acetone. The chemical scheme also treats the degradation of the aerosol precursor species: sulphur dioxide (SO_2); dimethylsulphide (DMS); and monoterpenes. In addition, two tracers are used to represent species which are used in aerosol nucleation and deposition processes: sulphuric acid (H_2SO_4) produced from the oxidation of SO_2 with the hydroxyl radical (OH); and a secondary organic species representing the condensable species from monoterpene oxidation. A scheme for the oxidation of SO_2 within clouds by dissolved hydrogen peroxide (H_2O_2) and ozone (O_3) is also provided to give sulphate production rates which are used for in-cloud aerosol growth rates.

2.4 Direct Radiative Effect and Forcing

Natural and anthropogenic aerosols exert a direct radiative effect (DRE) by scattering and absorbing incoming solar and outgoing long-wave radiation. The magnitude of the DRE depends on the atmospheric aerosol concentrations and their optical properties. The magnitude and sign of the DRE also depends on environmental factors such as the presence of clouds and the brightness of the underlying surface. A negative DRE

Mode name	Soluble ?	Radius Range (μm)	Components
Nucleation	Yes	$\bar{r} < 0.005$	SO ₄ , OC, OC ₂
Aitken	Yes	$0.005 < \bar{r} < 0.05$	SO ₄ , SS, BC, OC, OC ₂
Accumulation	Yes	$0.05 < \bar{r} < 0.5$	SO ₄ , SS, BC, OC, OC ₂ , DU
Coarse	Yes	$\bar{r} > 0.5$	SO ₄ , SS, BC, OC, OC ₂ , DU
Aitken	No	$0.005 < \bar{r} < 0.05$	BC, OC
Accumulation	No	$0.05 < \bar{r} < 0.5$	DU
Coarse	No	$\bar{r} > 0.5$	DU

Table 2: MODE aerosol scheme, with component species: SO₄, sulphate; SS, sea-salt; BC, Black Carbon; OC, Organic Carbon; OC₂, Organic Carbon from biogenic VOCs; DU, dust.

yields a loss of energy and a cooling of the climate system, counteracting greenhouse gas warming (Andreae et al., 2005). At the surface, the DRE is one component of the global dimming phenomenon, whereby incoming solar radiation is decreased by increased extinction through the atmosphere (Wild et al., 2008). It has also been suggested that the fraction of diffuse radiation reaching the surface, modulated in part by aerosol DRE, affects plant growth and the land carbon sink (Mercado et al., 2009). At the top of the atmosphere and in the shortwave spectrum, the DRE is typically negative as aerosols tend to increase the outgoing radiative flux. Absorbing aerosols, such as black carbon from fossil-fuel or biomass-burning emissions, when overlying bright surfaces, such as clouds, deserts or ice-covered surfaces, can exert a positive DRE. At the surface, all aerosol species exert a negative DRE. At the top of the atmosphere and in the longwave spectrum, only larger aerosols such as mineral dust have a significant effect on radiative fluxes. The longwave DRE is typically positive, as the aerosol layer is located at temperatures colder than the surface temperature. Estimates of the aerosol direct radiative effect due to present-day natural and anthropogenic aerosols range from -5 to -7 Wm^{-2} in the shortwave spectrum, and in clear-sky at the top of the atmosphere (Anderson et al., 2005). The DRE of anthropogenic aerosols, considered external to the climate system, is termed direct radiative forcing (DRF), and is defined by the IPCC with respect to pre-industrial conditions. The anthropogenic aerosol DRF is estimated at -0.4 Wm^{-2} with an error bar of $\pm 0.4 \text{ Wm}^{-2}$ by the latest IPCC assessment report (Forster et al., 2007).

In HadGEM, the DRE is diagnosed by differencing net radiative fluxes obtained by calling the radiation scheme twice. The first call includes scattering and absorption of radiation by aerosols; the second does not and is used for advancing the model into its next timestep. By doing so, surface and tropospheric temperatures are held fixed for the DRE calculation and the model evolution is unaffected by aerosols. The DRF is obtained from a pair of simulations, the first using present-day aerosol emissions, the other using 1860 aerosol emissions. Differences in net radiative fluxes yield the DRF exerted by the change in aerosol concentrations between 1860 and present-day.

A quantity closely related to the DRE is the extinction aerosol optical depth. Extinction is the sum of scattering and absorption of radiation at a given wavelength. The extinction aerosol optical depth (τ) is the column-integrated extinction defined as:

$$\tau = \int_z k_{ext}(\lambda)r(z)\rho(z)dz,$$

where λ is the wavelength, z is the vertical coordinate in m, k_{ext} is the specific extinction coefficient ($\text{m}^2 \text{kg}^{-1}$), r is the aerosol mass mixing ratio (kg kg^{-1}), and ρ is the air density (kg m^{-3}). The specific extinction coefficient varies with wavelength and water content of the aerosol. The optical depth is dimensionless, with typical values in the range 0 – 3. Aerosol optical depths for CLASSIC and MODE are now standard diagnostics from the model, and allow comparison with observations made from the surface and from satellite platforms.

It should be noted that the interaction between aerosols and radiation is implemented very differently for CLASSIC and MODE aerosols. CLASSIC aerosol components have prescribed size distributions and refractive indices, allowing offline calculations of aerosol optical properties. Water uptake by aerosols, termed hygroscopic growth, is prescribed as a function of relative humidity. In contrast, size distribution, water content, and refractive indices of MODE aerosols vary interactively during a simulation. Consequently, MODE aerosol optical properties have to be computed at runtime. These two ways of interacting with radiation co-exist, thus allowing CLASSIC mineral dust to be used with MODE aerosol species.

3 Experimental Design

The UKCA model was configured into the HadGEM3 climate model and a double call to the radiation scheme was made to allow the direct radiative effect to be diagnosed (see section 2.4). The code changes made incorporate the UKCA-MODE aerosol scheme contributed to the UKCA project by work done at Leeds University, and also includes work done at the Met Office to allow the aerosol concentrations from this scheme to interact with the radiation scheme in the Unified Model.

Five year simulations of the model with emissions appropriate for the years 1860 and 2000 have been made. Emissions for 1860 and 2000 are taken from those provided to support modelling activities for the Intergovernmental Panel on Climate Change (IPCC) fifth assessment report (AR5) described by Larmarque et al. (2010). For biomass burning emissions, grassfire emissions were added to the surface layer, and forest fires were assumed to be equally distributed between model levels two and twelve (approximately from 50 m to 3 km). Dimethylsulfide (DMS) emissions were estimated from the interactive scheme in the Unified Model, and used to drive both UKCA and CLASSIC. For each time horizon, two model runs were made to diagnose the direct radiative effect for each aerosol model.

4 Results

4.1 Atmospheric gas-phase constituents

Figure 1 shows the comparison between mean SO_2 mixing ratios for December, January and February at two heights. At 20 m, concentrations over the industrial source regions are similar, however UKCA has larger background concentrations, notably in

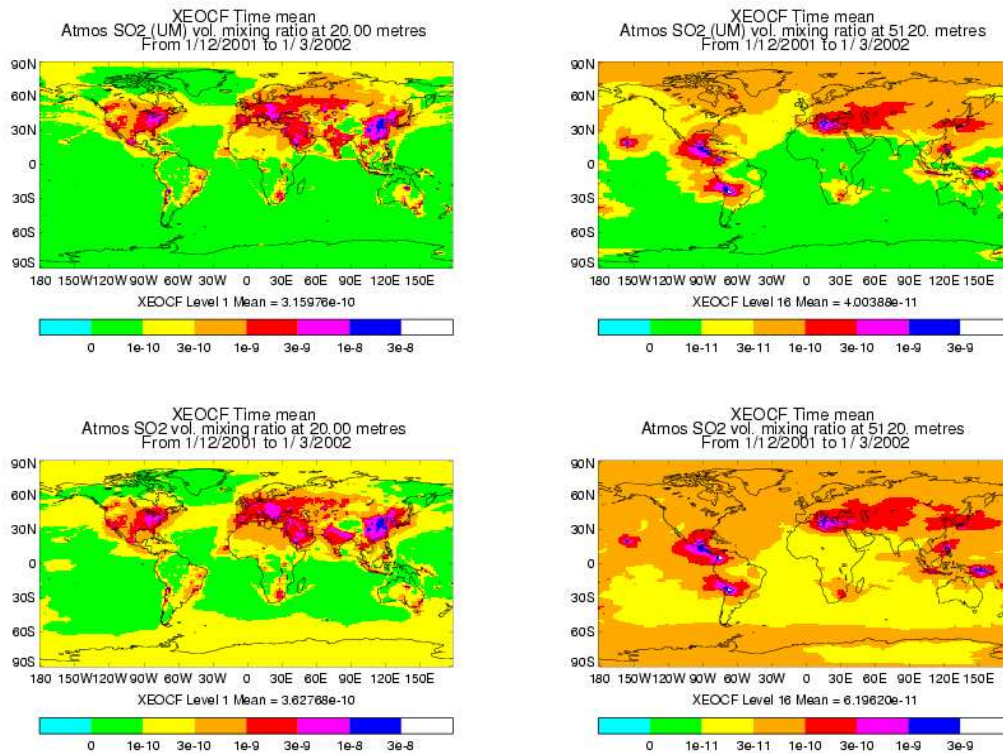


Figure 1: SO₂ concentrations from CLASSIC and UKCA simulations. Top row are CLASSIC simulations at 20m and 5120m, bottom row are for UKCA at the same heights. The results are the mean for December, January and February.

the southern hemisphere poleward of 60°S. At 5120 m, the UKCA simulation shows considerably higher concentrations, with global mean mixing ratio some 50 % higher. It is known that recent improvements to the DMS (dimethylsulfide) oxidation scheme (using rate coefficient from Karl et al. (2007)) in UKCA will produce more SO₂, and this is likely to produce the differences seen in remote regions where this source predominates.

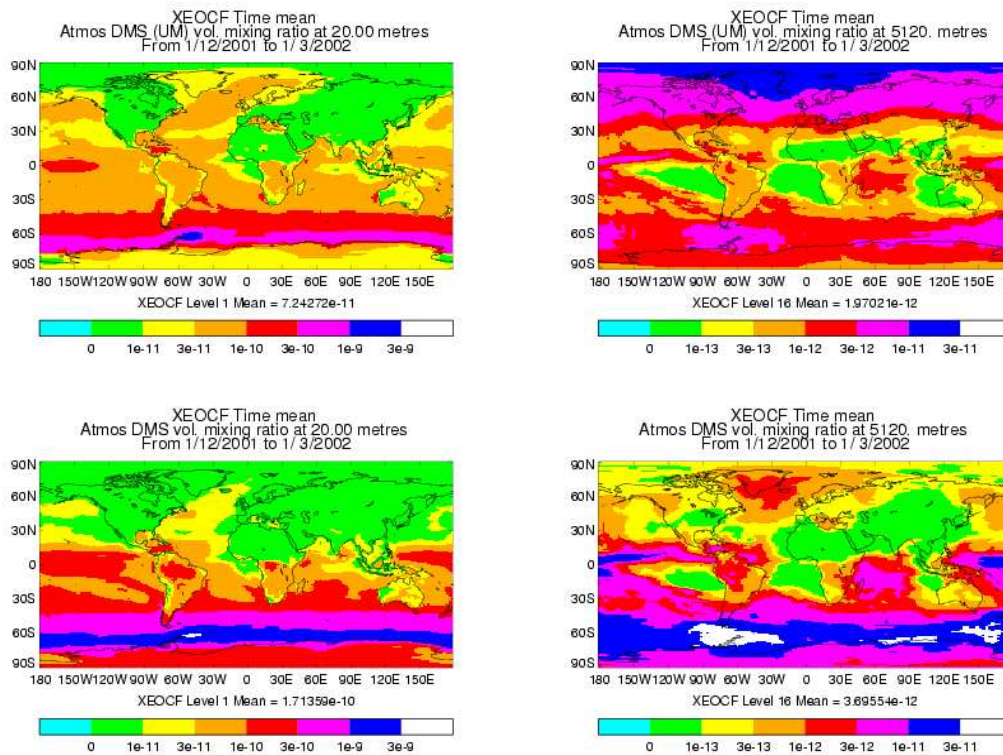


Figure 2: DMS concentrations from CLASSIC and UKCA simulations. Top row are CLASSIC simulations at 20m and 5120m, bottom row are for UKCA at the same heights. The results are the mean for December, January and February.

Figure 2 shows the comparison between mean DMS mixing ratios for December, January and February at two heights. At 20 m, concentrations in the northern hemisphere are considerably higher in CLASSIC. This is likely to be due to the lack of the reaction $\text{DMS} + \text{NO}_3$ in CLASSIC. In the southern hemisphere, where NO_3 concentrations are lower, UKCA has higher DMS concentrations. At 5120 m, these effects remain, with concentrations over the Arctic ocean around an order of magnitude higher in the CLASSIC simulation.

Figure 3 shows the comparison between SO₂ concentrations and observed surface concentrations (Hjellbrekke, 2003) for both models for June. The models tend overestimate SO₂ concentrations over Europe, and this is typical of other models (e.g. Berglen et al., 2007). There are several reasons for this discrepancy, and it is likely that oxidation mechanisms not included in current models are responsible.

Table 5 shows the normalised mean bias and correlation coefficient between the UKCA-MODE and CLASSIC results with the EMEP and CASTNET network observations for

December and June. The EMEP observations cover Europe, and CASTNET covers the United States of America. From these statistics, both models overestimate SO₂ concentrations. Normalised mean bias for UKCA-MODE is lower than for CLASSIC except for June in Europe, and the correlation coefficient is better in all four cases.

4.2 Sulphur oxidation and sulphate aerosol concentrations

Source or Loss	Flux UKCA 2000	Flux LMDZ 2000	Flux UKCA 1860
Industrial Emission	51.8	63.0	1.6
Natural Emission	7.4	7.8	7.4
DMS + OH \Rightarrow SO ₂	10.2	11.3	13.1
DMS + NO ₃ \Rightarrow SO ₂	4.7	5.2	1.7
Total Sources	74.1	91.9	23.7
SO ₂ + OH	12.2	14.0	4.3
HSO ₃ + H ₂ O ₂ (Aq)	15.8	27.9	6.1
SO ₃ + O ₃ (Aq)	10.2	21.1	2.0
Dry deposition	25.0	22.7	6.0
Wet deposition	11.0	6.2	5.3

Table 3: Annual SO₂ fluxes in UKCA and the LMDZ model (Boucher et al., 2002) for the year 2000. Units are Tg [S]/year. The total sources for the LMDZ model includes a contribution of 4.6 Tg/year from oxidation of H₂S and DMSO. Also shown are the results for UKCA for the year 1860.

It was not possible to compare the SO₂ oxidation schemes between CLASSIC and UKCA-MODE from the results of these simulations. However, here we compare the SO₂ budget from UKCA with the LMDZ simulation (Boucher et al., 2002). Table 3 shows the contributions to the sources and sinks of SO₂ compared to those for the LMDZ model. Note that the overall sources are less in the emission budget used in the present simulations for the year 2000 than used in the LMDZ model. The SO₂ produced from the oxidation of DMS is approximately the same in both models. The aqueous oxidation of SO₂ is proportionately less compared to the LMDZ model. Also shown is the SO₂ budget for the year 1860. Natural emissions dominate, and sulphate production was only 32 % of that in the present day. The fraction of SO₂ oxidised to sulphate aerosol was around 52 % in UKCA for both the 1860 and 2000 simulation. This suggests that simulated oxidant concentrations did not change significantly. Figure 4 shows annually-averaged sulphate aerosol concentrations versus observations at the surface. The CLASSIC model appears to underestimate sulphate at latitudes above 50 °N, probably because DMS oxidation does not include oxidation by the nitrate radical (NO₃) which is important in the winter when hydroxyl radical concentrations are low. Sulphate concentrations in UKCA-MODE are generally higher over the remote continental areas of the northern hemisphere compared to CLASSIC. This is likely to be due to a longer lifetime of sulphate in UKCA-MODE, due mainly to washout process differences.

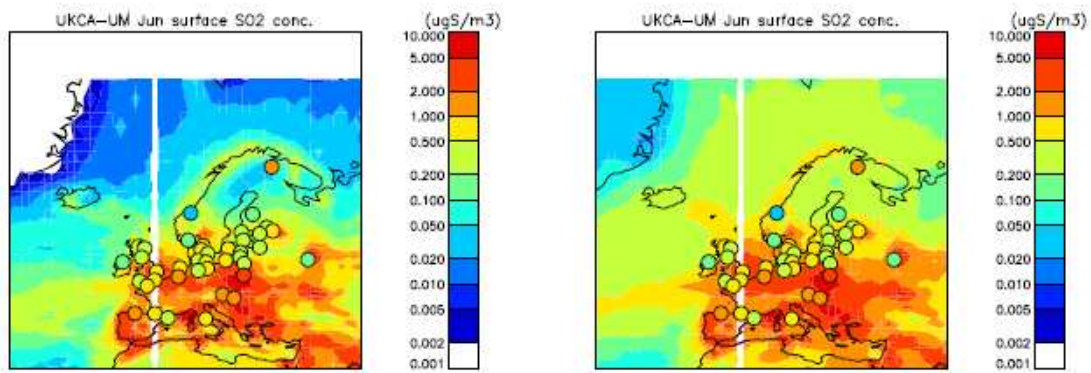


Figure 3: SO₂ concentrations from the CLASSIC (left) and UKCA-MODE (right) simulations compared to EMEP observations for June 2000.

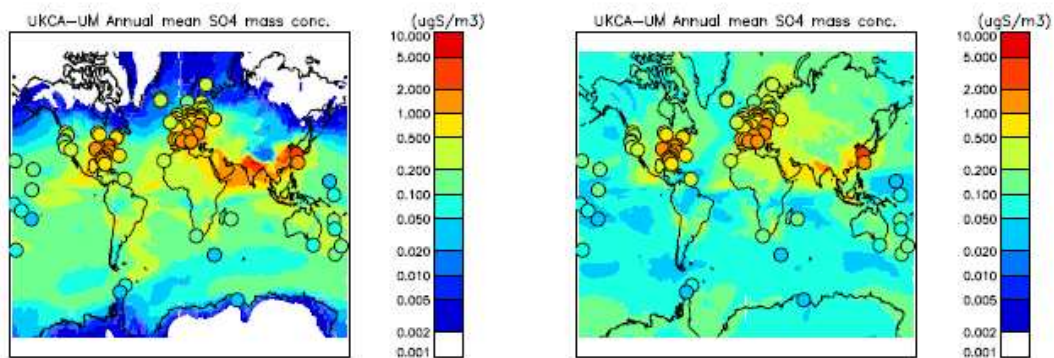


Figure 4: Annual mean sulphate aerosol concentrations from the CLASSIC (left) and MODE (right) simulations compared to observations.

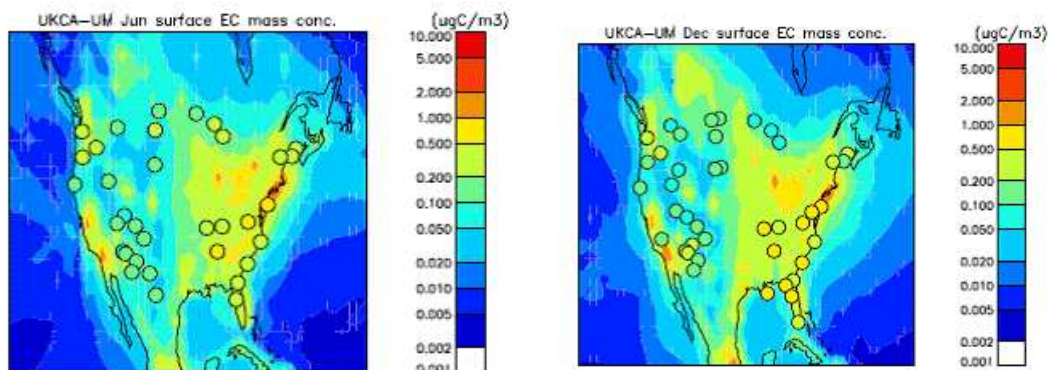


Figure 5: Black carbon aerosol concentrations from the UKCA simulation compared to IMPROVE observations for December (left) and June (right) 2000.

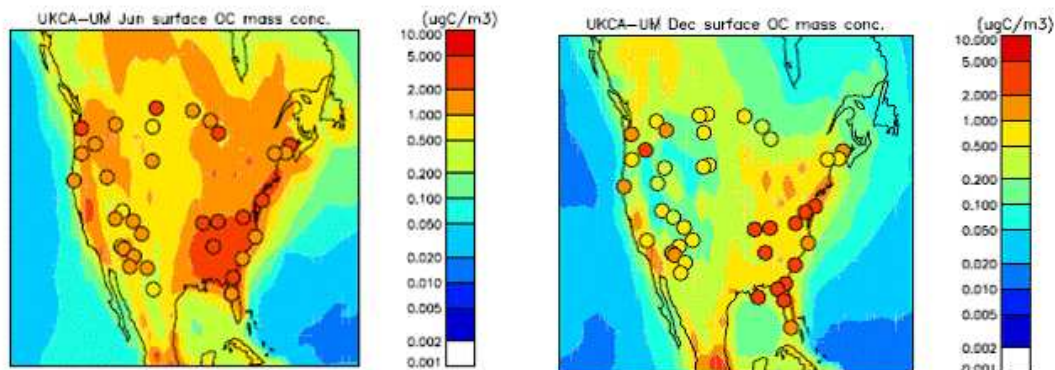


Figure 6: Organic carbon aerosol concentrations from the UKCA simulation compared to IMPROVE observations for December (left) and June (right) 2000.

4.3 Speciated aerosol mass and lifetime

Table 4 shows total mass and lifetime for the aerosol species simulated by CLASSIC and UKCA-MODE, averaged over the globe and over the 5 years of simulation. Standard deviation measures the variability in annual averages within those 5 years. The variability is small for all species except mineral dust (see below), which suggests that aerosol emissions dominate meteorology in determining the mass of aerosols in the atmosphere. Also shown are corresponding numbers from the AeroCom intercomparison of aerosol modelling in several chemical transport and general circulation models (Textor et al., 2006). AeroCom results are reported as the median of simulations by participating models. For the lifetime, the range of modelled values is also given.

For sulphate, the mass simulated by CLASSIC is less than that in UKCA-MODE and AeroCom and is a consequence of the underestimation of sulphate aerosol concentrations in CLASSIC, especially in winter. UKCA-MODE sulphate mass is closer to the AeroCom median. However, its lifetime appears too long: this is due to the relatively weak wet deposition rate of sulphate aerosols in UKCA-MODE.

Mineral dust, which comes from CLASSIC in both simulations, has about twice the mass given by the median of AeroCom models and is thus very likely to be overestimated. The large standard deviation shows the large variability in mineral dust mass from one year to the next, which is expected from a wind-blown aerosol that is very sensitive to the simulated climate.

For CLASSIC, black and organic carbon aerosols are for the fossil-fuel component only. The biomass-burning component is simulated as an independent tracer called biomass-burning aerosol. In contrast, UKCA-MODE and AeroCom consider black and organic carbon aerosols as the sum of fossil-fuel and biomass-burning components. Total carbonaceous aerosols compare well in both models, with a mass of 1.1 Tg. Both mass and life time are close to the AeroCom median and within the AeroCom range.

Figures 5 – 6 show examples of the comparison between model results from UKCA-MODE for black carbon and organic carbon aerosol components with the IMPROVE network (Malm et al., 1994) measurements for June, 2000. These comparisons are improved against previous results with this model and are now comparable with the

results from the off-line version of the MODE aerosol model. The improvements are likely to be due to use of better emission datasets in these simulations. Table 5 shows the normalised mean bias and correlation coefficient between the UKCA-MODE results and the IMPROVE network results. The results from CLASSIC are harder to interpret with these observations, as the biomass burning aerosol in this model contains both black and organic carbon.

Sea-salt mass in CLASSIC is very large and UKCA-MODE is a clear improvement with respect to the median of AeroCom models. Sea-salt is purely diagnostic in CLASSIC and since it is not transported, it does not have a lifetime. Sea-salt lifetime in UKCA-MODE is within the range simulated by models participating in AeroCom.

Species	CLASSIC	UKCA-MODE	AeroCom
	Total mass		
Sulphate	0.40 ± 0.01	0.67 ± 0.02	0.66
M. Dust	36.68 ± 6.74	35.71 ± 3.15	20.50
BC	0.19 ± 0.01	0.12 ± 0.01	0.21
OC	0.17 ± 0.01	0.99 ± 0.02	1.21
Biomass	0.74 ± 0.02		
Sea-salt	25.57 ± 0.08	4.80 ± 0.26	6.37
	Lifetime (days)		
Sulphate	3.3 ± 0.1	6.2 ± 0.1	4.1 (3.0–5.5)
M. Dust	1.1 ± 0.1	1.1 ± 0.1	4.0
BC	12.9 ± 0.2	5.6 ± 0.1	6.5 (5.2–15)
OC	4.7 ± 0.1	7.1 ± 0.2	6.2 (4.2–11)
Biomass	6.3 ± 0.2		
Sea-salt		0.2 ± 0.01	0.4 (0.2–1.0)

Table 4: Total mass and lifetime of aerosol species in CLASSIC, UKCA-MODE, and the median of the AeroCom intercomparison of aerosol modelling in numerical models (range given in brackets for lifetime). Sulphate mass is given in Tg[S]. Black carbon (BC), organic carbon (OC), and biomass-burning masses are given in Tg[C]. Mineral dust and sea-salt masses are given in Tg of mineral dust and NaCl, respectively. For CLASSIC, BC and OC refer to the fossil-fuel components only; the biomass-burning component is given under biomass. For UKCA-MODE and AeroCom, BC and OC refer to the combination of fossil-fuel and biomass-burning components.

4.4 Comparison between aerosol optical depths

Figure 7 shows seasonal distributions of total aerosol optical depth at $0.55 \mu\text{m}$ as simulated by HadGEM3 using CLASSIC or MODE aerosols, and as retrieved by the Moderate Resolution Imaging Spectroradiometer (MODIS) satellite instrument on NASA’s Terra platform (Remer et al. 2005). MODIS distributions are multiyear seasonal means for the period 2002–2006, using collection 5 data. Modelled distributions are multiyear seasonal means for the 5 years of the CLASSIC and MODE simulations.

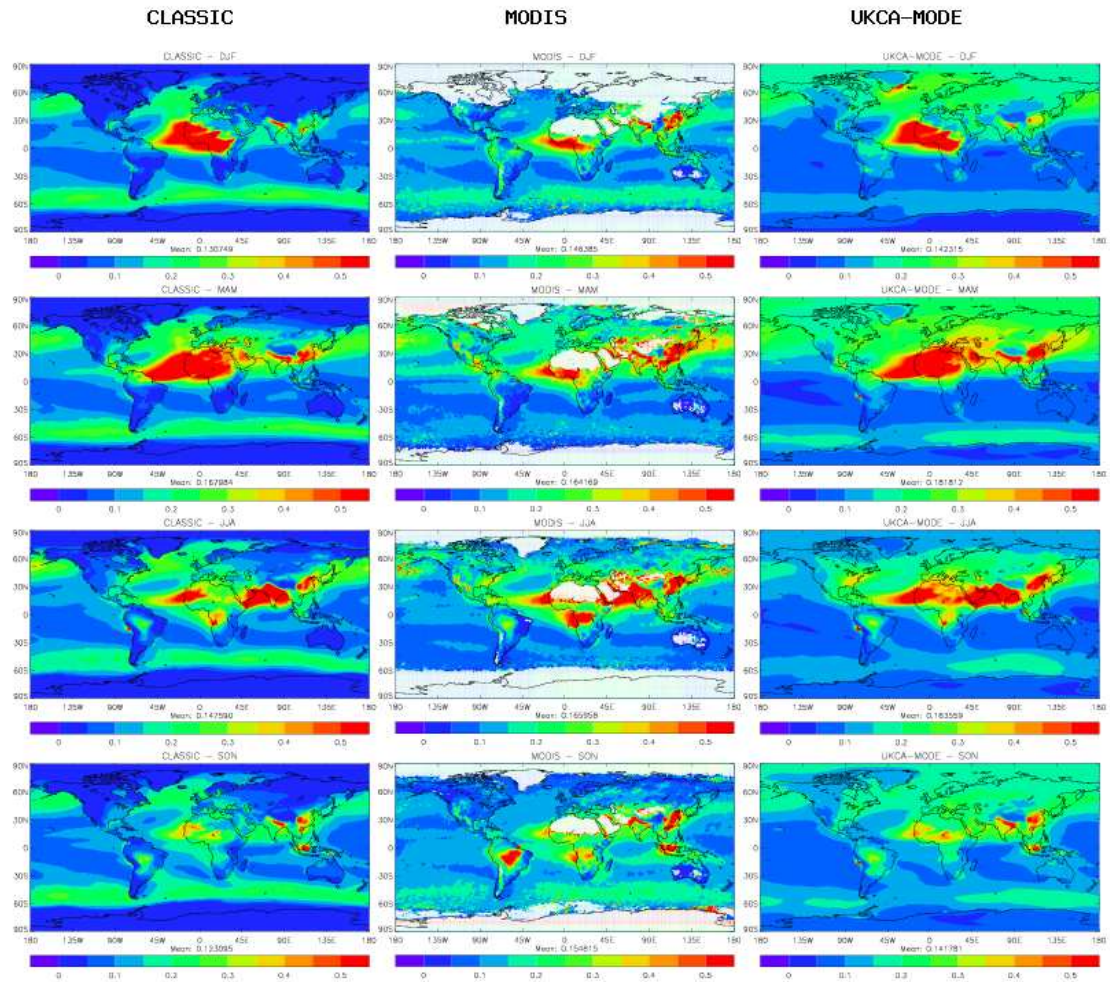


Figure 7: Seasonal distributions of the total aerosol optical depth at $0.55 \mu\text{m}$ as simulated by CLASSIC (left), retrieved from MODIS observations (centre), and simulated by MODE (right).

Species	Month	Observations	CLASSIC	MODE	CLASSIC	MODE
			Normalised	mean bias	Correlation coefficient	
SO ₂	Dec	EMEP	2.81	2.75	0.52	0.69
SO ₂	Jun	EMEP	2.76	3.83	0.69	0.70
SO ₂	Dec	CASTNET	4.71	3.42	0.74	0.89
SO ₂	Jun	CASTNET	2.12	2.02	0.69	0.74
SO ₄	Dec	EMEP	-0.53	-0.36	0.67	0.35
SO ₄	Jun	EMEP	0.77	-0.29	0.58	0.66
SO ₄	Dec	IMPROVE	-0.20	-0.40	0.86	0.89
SO ₄	Jun	IMPROVE	0.25	-0.37	0.88	0.81
BC	Dec	IMPROVE		-0.07		0.57
BC	Jun	IMPROVE		-0.10		0.54
OC	Dec	IMPROVE		-0.66		0.49
OC	Jun	IMPROVE		-0.16		0.62

Table 5: Normalised mean bias and correlation coefficient against surface observations. Species included are: sulphur dioxide, SO₂; sulphate aerosol, SO₄; black carbon, BC; and organic carbon, OC. Observation datasets used are: EMEP, (Hjellbrekke, 2002); CASTNET, (Mueller, 2003); IMPROVE, (Malm, 1994).

Both aerosol models reproduce the main patterns of aerosol distributions. Large optical depths due to sea-salt can be seen around the ocean at 50 °N and 50°S. Transports of windblown mineral dust from the Sahara across the Atlantic and from China across the Pacific are also reproduced. Mineral dust optical depths are however overestimated in Spring, a consequence of the large mineral dust mass simulated. Industrialised countries of North America, Europe, and Asia are associated with large optical depths in summer when atmospheric chemical reactions are more efficient. Large aerosol optical depths in Southern Africa and South America are due to seasonal biomass-burning activities, and both models underestimate the optical depth there. The main cause for this is the strong interannual variation in biomass-burning aerosol emissions. The MODIS period includes 2003 and 2006, which were exceptionally active years for biomass-burning activities. In contrast, emission datasets used by CLASSIC and MODE represent average present-day conditions and lead to lower optical depths. There are significant differences between CLASSIC and MODE, however. CLASSIC clearly struggles at producing aerosol optical depth over North Hemisphere continents in all seasons. MODE is therefore an obvious improvement, although it does overestimate optical depths in the North Hemisphere in winter and spring. The long lifetime of UKCA-MODE sulphate is likely to be responsible for this overestimation, allowing sulphate aerosols to be transported too far. Another reason for differences between the two models is that UKCA-MODE has sea-salt aerosol scheme which allows sea-salt aerosol to be advected over land areas. This is a significant effect over some areas, notably over north-west Europe as seen in figure 8. Sea-salt aerosol optical depth is overestimated by CLASSIC and underestimated by MODE, especially in winter. Satellite retrievals of aerosol optical depth are uncertain and only sample a fraction of the cloud-free surface of the Earth. Different satellite instruments yield different statistics (Mishchenko *et al.*, 2007). For a more quantitative assessment of the

model performance, we therefore turn to the ground-based sun-photometer network AERONET (Aerosol Robotic Network, Holben et al., 2001). A climatology of seasonal optical depths at $0.44 \mu\text{m}$ covering 67 sites worldwide and the period 1998-2002, which brackets the year 2000 simulated by HadGEM3, is used to compute root-mean square (RMS) errors for CLASSIC and UKCA-MODE simulations. Results shown in Table 6 suggest smaller RMS errors for MODE in all seasons, confirming the overall improvement in simulated aerosol optical depths when MODE is used.

Season	CLASSIC	UKCA-MODE
DJF	0.107	0.094
MAM	0.151	0.147
JJA	0.138	0.127
SON	0.122	0.104

Table 6: Seasonal root-mean square errors between aerosol optical depths at $0.44 \mu\text{m}$ from AERONET measurements at 67 sites for 1998-2002 and CLASSIC or UKCA-MODE simulations for the year 2000.

Figure 8 shows distributions of aerosol optical depths at $0.44 \mu\text{m}$ simulated by CLASSIC and MODE for North Hemisphere summer, with the AERONET climatology for that season overplotted as coloured squares centred on the AERONET site location. Where coloured squares match the background distribution, the simulation agrees well with AERONET. In summer, CLASSIC compares reasonably well against AERONET, but MODE still outperforms, especially in Europe, Africa, and the Eastern United States. MODE overestimates optical depths in the Western U.S., however.

4.5 Comparison of direct radiative effect

Figure 9 shows distributions of the shortwave DRE due to all simulated aerosols. The DRE is computed with respect to an atmosphere that contains no aerosols, and is shown for all-sky (including clouds) and clear-sky (excluding clouds) conditions at the top of the atmosphere, and for clear-sky conditions at the surface. Variability of the global mean is computed as the standard deviation over annual means for the 5 simulated years. CLASSIC and MODE share similar distributions of the DRE. The DRE is weaker in CLASSIC as CLASSIC aerosol optical depths are smaller. MODE exhibits positive all-sky forcing off the shores of Namibia where biomass-burning aerosols overlie stratocumulus clouds. CLASSIC gets weak negative forcing in that region, suggesting that CLASSIC biomass-burning aerosols are less absorbing than their MODE counterparts.

Table 7 summarises the global-, annual-averaged DREs for CLASSIC and MODE shown on Figure 9. It also includes the atmospheric shortwave DRE in clear-sky, computed as the difference between DRE at the top of the atmosphere and the surface. The atmospheric DRE measures the amount of energy absorbed by the aerosol layer and is similar in CLASSIC and MODE, suggesting that those models share similar aerosol absorption properties on a global scale. The table also shows radiative forcing efficiencies (RFEs) for top of atmosphere and surface clear-sky DREs. The RFE is a measure of the forcing exerted per unit aerosol optical depth and is computed as the ratio between

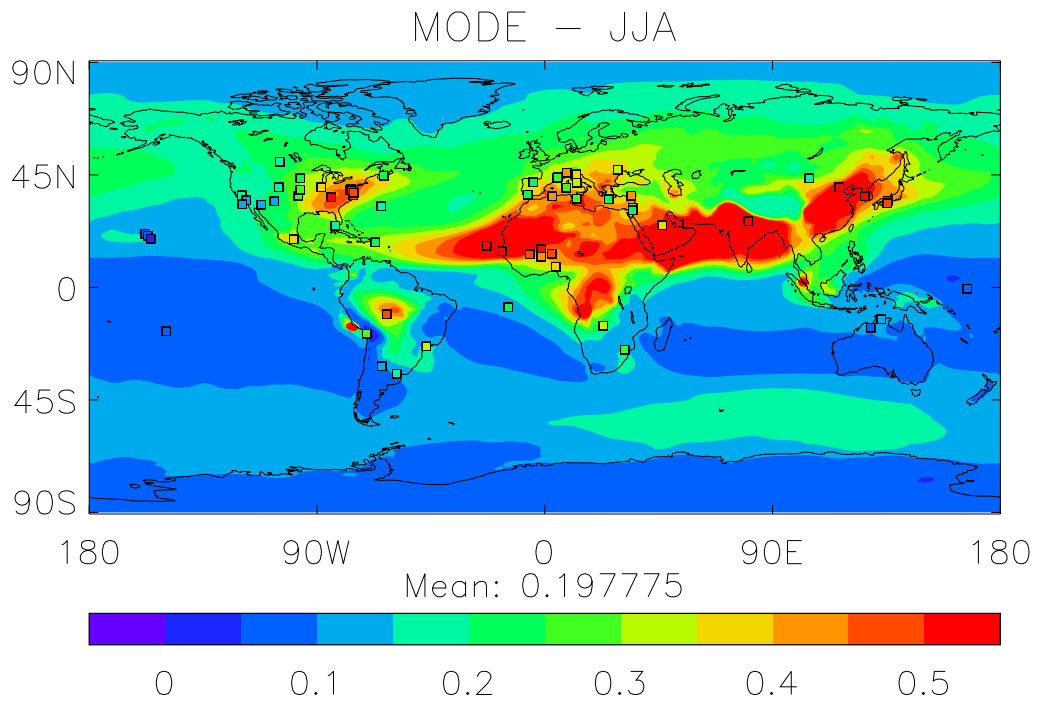
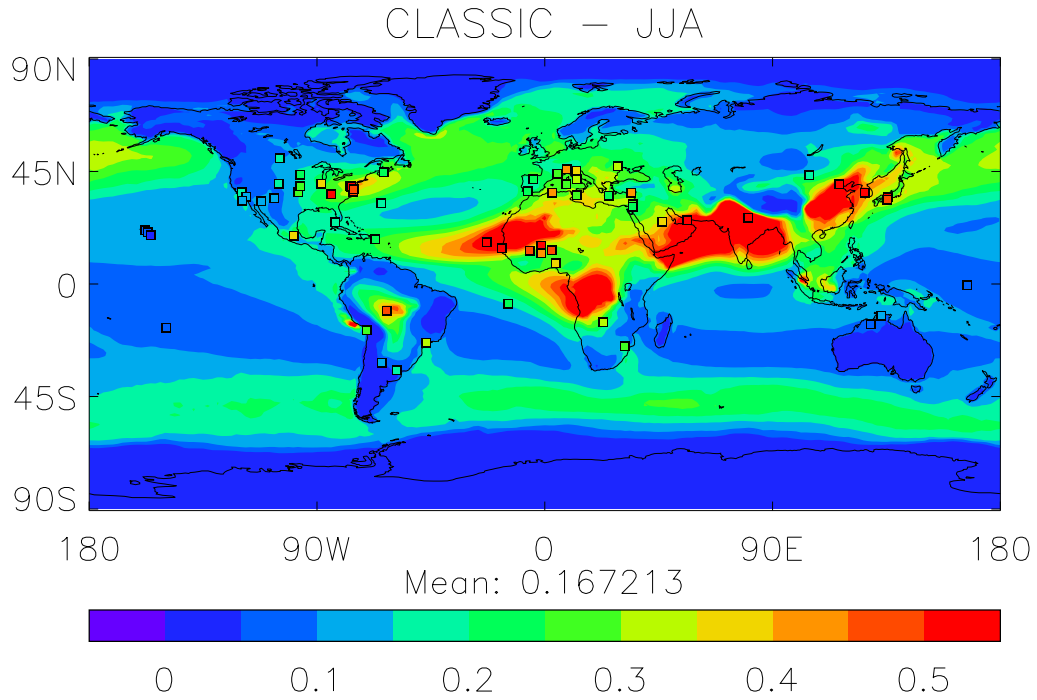


Figure 8: Distributions of the total aerosol optical depth at $0.44 \mu\text{m}$ as simulated by CLASSIC (top) and MODE (bottom) for the months of June-July-August (JJA). Coloured squares represent JJA means for 1998-2002 at AERONET sun-photometer sites.

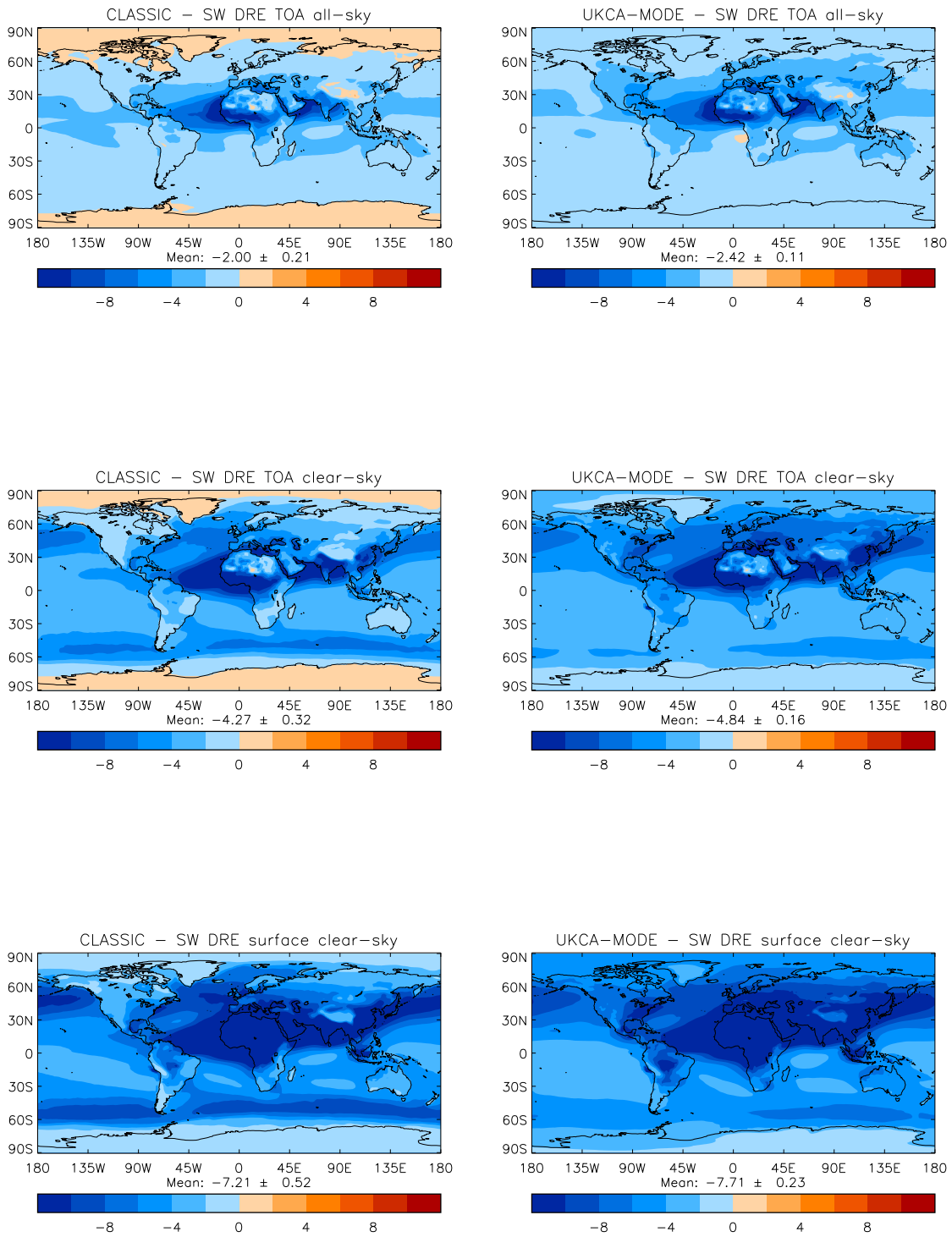


Figure 9: Annual distributions of shortwave direct radiative effect (SW DRE, in Wm^{-2}) due to all present-day aerosols simulated by CLASSIC (left) and MODE (right). DRE is computed at the top of the atmosphere for all-sky (top) and clear-sky (middle) conditions, and at the surface for clear-sky conditions (bottom).

global-, annual-averaged DRE and aerosol optical depth. CLASSIC and MODE have virtually the same RFEs. This is a very positive result, showing that the completely different ways of interacting with radiation implemented in CLASSIC and MODE are consistent.

	CLASSIC	MODE
Total AOD	0.142	0.157
SW DRE TOA all-sky	-2.00 ± 0.21	-2.42 ± 0.11
SW DRE TOA clear-sky	-4.27 ± 0.32	-4.84 ± 0.16
SW DRE surface clear-sky	-7.21 ± 0.52	-7.71 ± 0.23
SW DRE atmos. clear-sky	+2.94	+2.87
SW RFE TOA clear-sky	-30.1	-30.8
SW RFE surface clear-sky	-50.8	-49.1

Table 7: Global and annual averaged aerosol optical depth (AOD, at $0.55 \mu\text{m}$), direct radiative effect (DRE, in Wm^{-2} and in the shortwave spectrum), and radiative forcing efficiency (RFE) for CLASSIC and MODE simulations. TOA stands for top-of-atmosphere.

In the longwave (not shown), the DRE is dominated by mineral dust which is modelled in the same way by both CLASSIC and MODE. The longwave DRE at the top of the atmosphere is $+0.9 \text{Wm}^{-2}$.

The anthropogenic DRF is exerted by changes in aerosol optical depth between 1860 and present-day conditions. It is obtained by differencing DREs obtained by the present-day and 1860 simulations of HadGEM3. Unfortunately, technical issues prevented present-day and 1860 simulations from maintaining parallel meteorology, and DRF estimates are contaminated by changes in natural aerosol concentrations.

4.6 Number concentrations

As the CLASSIC aerosol scheme assumes a fixed size distribution for each aerosol model, and therefore aerosol mass and number are directly related, we expect UKCA-MODE to deliver a better estimate of aerosol number concentrations. This is because it directly simulates aerosol number so that aerosol size is no longer fixed. Aerosol indirect effects on clouds are strongly linked to aerosol number concentration, and we therefore anticipate that UKCA-MODE will improve the simulation of these effects. Figure 10 shows simulated cloud condensation nuclei number concentrations against available measurements made in a wide range of conditions. It is clear that UKCA-MODE shows a clear improvement over CLASSIC, with the majority of the results falling within a factor of two of the observations.

5 Conclusions

The UKCA-MODE model of global aerosol components is compared to the CLASSIC model and evaluated with the available measurements. The simulations used the same emission datasets and were done simultaneously within the same climate model. The

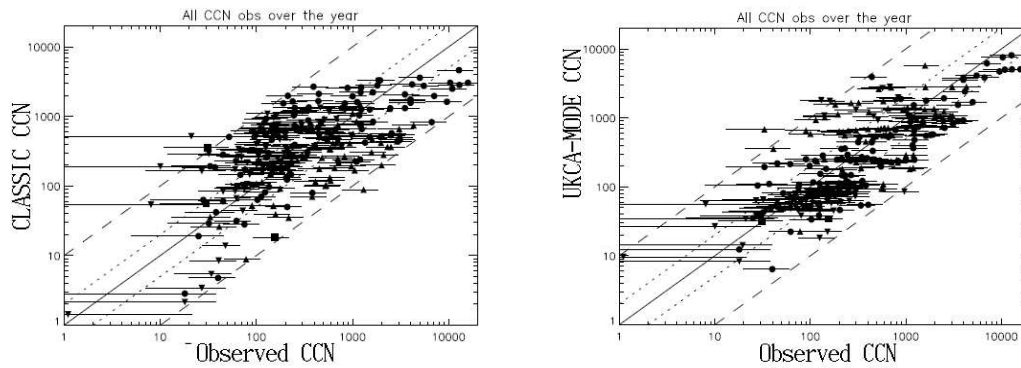


Figure 10: Cloud condensation nuclei concentrations (cm^{-3}) predicted by CLASSIC (left) and UKCA-MODE (right) compared with observations (Spracklen, 2009). The symbols are: \blacksquare , northern hemisphere polar; \bullet , northern hemisphere mid-latitudes; \blacktriangle , tropics; \blacktriangledown , southern hemisphere mid-latitudes; \blacklozenge , southern hemisphere polar.

comparison with observations for UKCA-MODE was better than in previous simulations using this model, probably because of improvements to the emission datasets used. There are clear improvements to the simulation of aerosol optical depth in UKCA-MODE when compared to CLASSIC, for example the root mean square errors in seasonal AOD are all less in UKCA-MODE (section 4.4).

There were differences between UKCA-MODE and CLASSIC in sulphate aerosol distributions (section 4.2 and 4.3), and these relate to differences between the oxidation of SO_2 and dimethylsulphide, as well as the removal of sulphate aerosol by wet deposition. The treatment of wet deposition in UKCA-MODE may be improved with a sub-grid scale treatment of aerosol washout, and re-evaporation of rainfall needs to be considered in this scheme. The improvement of the current operator splitting of washout and transport from convection in this model forms the topic of research at Oxford University, and should also improve the model. The rather low production of sulphate aerosol through the aqueous chemistry in comparison with the off-line version of UKCA-MODE needs to be attributed to differences in the chemical scheme used or with the differences in the simulation of clouds.

The aerosol optical depth from UKCA-MODE was around 10 % higher than from CLASSIC, and this was attributed mainly to an increased sulphate aerosol concentrations over the northern hemisphere continents, although the advection of sea-salt aerosol in UKCA-MODE is also important in some areas. The results reported here are the first which use the direct radiation forcing coupling of UKCA-MODE to the MetUM radiation schemes. Despite the differences in the radiative forcing calculations between the two models the radiative forcing per unit AOD was similar for both aerosol models. Work to use UKCA-MODE results to predict aerosol indirect effects on cloud albedo and precipitation is in progress at Oxford University.

UKCA-MODE development is proceeding, with the addition of mineral dust, ammonium, and nitrate aerosols. The UKCA-MODE model has been developed at Leeds University using a chemical transport model, and the aerosol results have been comprehensively evaluated against a large range of observations. The intercomparison between

these two models brings greater confidence in simulated aerosols in HadGEM3, but is not reported here for reasons of space.

References

- Anderson, T.L. *et al.*, An A-Train strategy for quantifying direct climate forcing by anthropogenic aerosols, *Bull. Amer. Meteorol. Soc.*, **12**, 1795–1809, 2005.
- Andreae, M.O., Jones, C.D. and Cox, P.M., Strong present-day aerosol cooling implies a hot future, *Nature*, **435**, 1187–1190, 2005.
- Arakawa, A. and Lamb, V.R., Computational design of the basic dynamical processes of the UCLA general circulation model, *Methods Comput. Phys.*, **17**, 173–265, 1977.
- Bellouin, N., Boucher, O., Haywood, J., Johnson, C., Jones, A., Rae, J., and Woodward, S., *Improved Representation of Aerosols for HadGEM2*, Hadley Centre Technical Note 73, 2007.
- Berglen, T.F., Myhre, G., Isaksen, I.S.A., Vestreng, V., and Smith, S.J., Sulphate trends in Europe: are we able to model the recent observed decrease?, *Tellus, B.*, **59**, 773–786, 2007.
- Boucher, O., Pham, M., and Venkataraman, C., *Simulation of the atmospheric sulfur cycle in the Laboratoire de Météorologie Dynamique General Circulation Model. Model description, Model Evaluation, and Global and European Budgets*, Institut Pierre Simon Laplace, Note No. 23, 2002.
- Davies, T., Cullen, M.J.P., Malcolm, A.J., Mawson, M.H., Staniforth, A., White, A.A., and Wood, N., A new dynamical core for the Met Office's global and regional modelling of the atmosphere, *Q. J. R. Meteorol. Soc.*, **131**, 1759–1782, 2005.
- Forster, P. *et al.*, Changes in atmospheric constituents and in radiative forcing, Chapter 2 of the IPCC fourth assessment report, 2007.
- Gregory, D. and Rowntree, P.R., A mass flux scheme with representation of cloud ensemble characteristics and stability-dependent closure, *Mon. Wea. Rev.*, **118**, 1483-1506, 1990.
- Holben, B.N. *et al.*, An emerging ground-based aerosol climatology: Aerosol optical depth from AERONET, *J. Geophys. Res.*, **106**, 9807–9826, 2001.
- Hjellbrekke, A.-G. *Data Report 2000, Acidifying and eutrophying compounds, Part 2, Monthly and Seasonal Summaries*, EMEP/CCC-Report 7/2002, Norwegian Institute for Air Research, 2002.
- Jacobson, M. Z., Tabazadeh A. and Turco, R. P., Simulating equilibrium within aerosols and nonequilibrium between gases and aerosols, *J. Geophys. Res.*, **101**, 9079-9091, 1996.
- Jones, A., Roberts, D.L., Woodage, M.J., and Johnson, C.E., Indirect sulphate aerosol forcing in a climate model with an interactive sulphur cycle, *J. Geophys. Res.*,

106, 20293-20310, 2001.

Karl, M., Gross, A., Leck, C., and Pirjola, L., Intercomparison of dimethylsulfide oxidation mechanisms for the marine boundary layer, *J. Geophys. Res.*, **112**, D15, doi:10.1029/2006JD007914, 2007.

Lamarque, J.-F., T.C. Bond, V. Eyring, C. Granier, A. Heil, Z. Klimont, D. Lee, C. Liou, A. Mieville, B. Owen, M. G. Schultz, D. Shindell, S. J. Smith, E. Stehfest, J. Van Aardenne, O. R. Cooper, M. Kainuma, N. Mahowald, J. R. McConnell, V. Naik, K. Riahi, and D.P. van Vuuren, Historical (1850–2000) gridded anthropogenic and biomass burning emissions of reactive gases and aerosols: methodology and application, *Atm. Chem. Phys. Disc.*, **10**, 4963–5019, 2010.
(www-atmos-chem-phys-discuss.net/10/4963/2010/)

Lock, A.P., Brown, A.R., Bush, M.R., Martin, G.M., and Smith, R.N.B., A new boundary layer mixing scheme. Part I: Scheme description and single-column model tests, *Mon. Wea. Rev.*, **128**, 3187–3199, 2000.

Malm, W. C., Sisler, J.F., Huffman, Eldred, D.R.A., and Cahill, T.A., Spatial and seasonal trends in particle concentration and optical extinction in the United States, *J. Geophys. Res.*, **99**, 1347–1370, 1994.

Manktelow, P.T., Mann, G.W., Carslaw, K.S., Spracklen, D.V., and Chipperfield, M.P., Regional and global trends in sulfate aerosol since the 1980s, *Geophys. Res. Lett.*, **34**, L14803, doi:10.1029/2006GL028668, 2007.

Mann, G.W., Carslaw, K.S., Spracklen, D.V., Ridley, D.A., Manktelow, P.T., Chipperfield, M.P., Pickering, S.J., and Johnson, C.E., Description and evaluation of GLOMAP-MODE: A modal global aerosol microphysics model for the UKCA composition-climate model. *in prep.*, 2010.

Mercado, L., Bellouin, N., Boucher, O., Sitch, S., Huntingford, C., Wild, M., and Cox, P., Impact of changes in diffuse radiation on the global land carbon sink, *Nature*, **458**, 1014–1017, doi:10.1038/nature07949, 2009.

Mishchenko, M.I., *et al.*, Past, present, and future of global aerosol climatologies derived from satellite observations: A perspective, *J. Quant. Spectro. Rad. Trans.*, **106**, 325–347, 2007.

Morgenstern, O., Braesicke, P., O'Connor, F.M., Bushell, A.C., Johnson, C.E., Osprey, S.M., and Pyle, J.A., Evaluation of the new UKCA climate–composition model. Part 1: The Stratosphere, *Geosci. Model Dev.*, **2**, 43–57, 2009.

Mueller, S.F., Seasonal Aerosol Sulfate Trends for selected regions of the United States, *J. of Air and Waste Management Ass.*, **53**, 168–184, 2003.

Rae, J.G.L., Johnson, C.E., Bellouin, N., Boucher, O., Haywood, J.M., and Jones, A., Sensitivity of global sulphate aerosol production to changes in oxidant concentrations and climate, *J. Geophys. Res.*, **112**, D10312, doi:10.1029/2006JD007826, 2007.

Remer, L.A. *et al.*, The MODIS aerosol algorithm, products, and validation, *J. Atmos. Sci.*, **62**, 947–973, 2005.

Solomon, S., Qin, D., Manning, M., Marquis, M., Averyt, K., Tigner, M.M.B., LeRoy Miller, H., and Chen, Z., *Climate Change 2007: The Physical Science Basis*, Cambridge University Press, 2007.

Spracklen, D. *Personal communication*, Leeds University, 2009.

Stokes, R.H. and Robinson, R.A., Interactions in aqueous non-electrolyte solutions: I. Solute-solvent equilibria. *J. Phys. Chem.*, **70**, 2126-2130, 1966.

Tang, I.N., and Munkelwitz, H.R., Water activities, densities, and refractive indices of aqueous sulfates and sodium nitrate droplets of atmospheric importance, *J. Geophys. Res.*, **99**, 18801-18808, 1994.

Textor, C., *et al.*, Analysis and quantification of the diversities of aerosol life cycles within AeroCom, *Atmos. Chem. Phys.*, **6**, 1777–1813, 2006.

Vignati, E.J., Wilson, J., and Stier, P., M7: An efficient size-resolved aerosol microphysics module for large-scale aerosol transport models, *J. Geophys. Res.*, **109**, D22202, doi:10.1029/2003JD004485, 2004.

Wild, M., Global dimming and brightening: A review, *J. Geophys. Res.*, **114**, D00D16, doi:10.1029/2008JD011470, 2009.

Woodward, S., Modelling the atmospheric life cycle and radiative impact of mineral dust in the Hadley Centre climate model, *J. Geophys. Res.*, **106**, 18155-18166, 2001.